Freshwater Input and Vertical Mixing in the Canada Basin's Seasonal Halocline: 1975 versus 2006–12

ERICA ROSENBLUM,[a] JULIENNE STROEVE,[a,b,c] SARAH T. GILLE,[d] CAMILLE LIQUE,[e] ROBERT FAJBER,[f] L. BRUNO TREMBLAY,[g] RYAN GALLEY,[h] THIAGO LOUREIRO,[i] DAVID G. BARBER,[a] AND JENNIFER V. LUKOVICH[a]

[a] *Centre for Earth Observation Science, University of Manitoba, Winnipeg, Manitoba, Canada*
[b] *Centre for Polar Observation and Modelling, Earth Sciences, University College London, London, United Kingdom*
[c] *National Snow and Ice Data Center, Cooperative Institute for Research in Environmental Sciences, University of Colorado Boulder, Boulder, Colorado*
[d] *Scripps Institution of Oceanography, University of California, San Diego, La Jolla, California*
[e] *Univ. Brest, CNRS, IRD, Ifremer, Laboratoire d'Océanographie Physique et Spatiale, IUEM, Brest, France*
[f] *Department of Physics, University of Toronto, Toronto, Ontario, Canada*
[g] *Department of Atmospheric Science, McGill University, Montreal, Quebec, Canada*
[h] *Department of Environment and Geography, University of Manitoba, Winnipeg, Manitoba, Canada*
[i] *Ryerson University, Toronto, Ontario, Canada*

(Manuscript received 1 June 2021, in final form 8 February 2022)

ABSTRACT: The Arctic seasonal halocline impacts the exchange of heat, energy, and nutrients between the surface and the deeper ocean, and it is changing in response to Arctic sea ice melt over the past several decades. Here, we assess seasonal halocline formation in 1975 and 2006–12 by comparing daily, May–September, salinity profiles collected in the Canada Basin under sea ice. We evaluate differences between the two time periods using a one-dimensional (1D) bulk model to quantify differences in freshwater input and vertical mixing. The 1D metrics indicate that two separate factors contribute similarly to stronger stratification in 2006–12 relative to 1975: 1) larger surface freshwater input and 2) less vertical mixing of that freshwater. The larger freshwater input is mainly important in August–September, consistent with a longer melt season in recent years. The reduced vertical mixing is mainly important from June until mid-August, when similar levels of freshwater input in 1975 and 2006–12 are mixed over a different depth range, resulting in different stratification. These results imply that decadal changes to ice–ocean dynamics, in addition to freshwater input, significantly contribute to the stronger seasonal stratification in 2006–12 relative to 1975. These findings highlight the need for near-surface process studies to elucidate the impact of lateral processes and ice–ocean momentum exchange on vertical mixing. Moreover, the results may provide insight for improving the representation of decadal changes to Arctic upper-ocean stratification in climate models that do not capture decadal changes to vertical mixing.

KEYWORDS: Ocean; Arctic; Ocean dynamics; Mixed layer; Seasonal variability; Multidecadal variability

1. Introduction

The surface waters of the Arctic Ocean have changed dramatically over the past several decades as a result of the diminishing sea ice cover that once shielded much of the ocean from wind and sunlight across all seasons (Perovich 2011; Stroeve and Notz 2018; Polyakov et al. 2020), and this has important consequences for the exchange of heat and nutrients between the surface and deeper ocean (McLaughlin et al. 2011; Carmack et al. 2015; Timmermans and Marshall 2020; Brown et al. 2020). Changes in Arctic sea ice conditions are generally thought to either strengthen or weaken the underlying upper-ocean stratification depending on the competing effects of freshwater input and of vertical mixing (Peralta-Ferriz and Woodgate 2015; Lique 2015; Nummelin et al. 2015; Davis et al. 2016). A now warmer atmosphere and ocean delays ice freeze-up, reduces winter ice growth, and can melt more sea ice each spring and summer, potentially releasing more fresh, buoyant meltwater to the surface (Stroeve et al. 2014; Carmack et al. 2016) and stabilizing the upper ocean. Conversely, the wind acts on a now more mobile ice pack (Hakkinen et al. 2008; Rampal et al. 2009; Spreen et al. 2011; Galley et al. 2013; Kwok et al. 2013; Brown et al. 2020), potentially generating greater shear that stirs and mixes the underlying ocean, and reducing the stability of the upper ocean (Lemke and Manley 1984; Polyakov et al. 2020). Increased stratification has been documented in recent decades in many regions of the Arctic, but the evolving relationship between freshwater input and upper-ocean vertical mixing in response to Arctic sea ice retreat remains an open question.

We examine this question by comparing the seasonal evolution of the upper-ocean salinity below sea ice during two time periods that are separated by approximately three decades,

Denotes content that is immediately available upon publication as open access.

Supplemental information related to this paper is available at the Journals Online website: https://doi.org/10.1175/JPO-D-21-0116.s1.

Corresponding author: Erica Rosenblum, erica.rosenblum@umanitoba.ca

DOI: 10.1175/JPO-D-21-0116.1

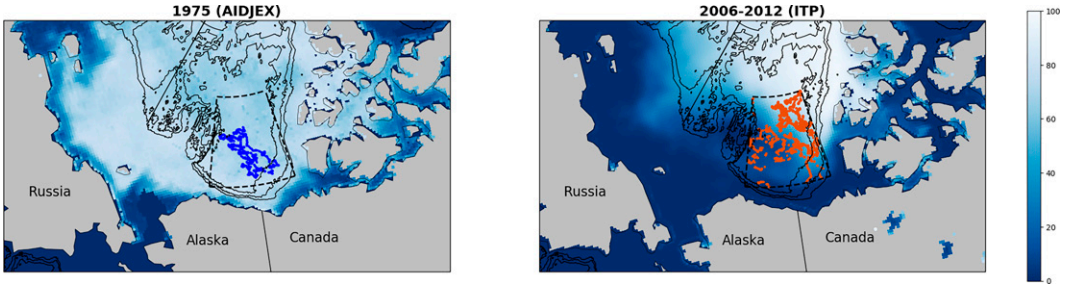

FIG. 1. Map of Canada Basin showing September sea ice concentration and location of ocean observations. (left) September 1975 mean sea ice concentration and location of measurements from AIDJEX sea ice camps (blue dots) and (right) 2006–12 September mean sea ice concentration and location of ITP observations (red dots). Region indicated by dashed lines shows the Canada Basin, which we define as the region bounded by 72°N, 80°N, 130°W, and 155°W. Solid lines indicate bathymetric contours at 1000, 2000, and 3000 m. The regional map of September 1975 sea ice concentrations is provided by *Nimbus-5* ESMR Polar Gridded Sea Ice Concentrations, Version 1 (Parkinson et al. 2004).

and that are associated with distinctly different sea ice conditions. The datasets come from the 1975 Arctic Ice Dynamics Joint Experiment (AIDJEX) program (Untersteiner et al. 2007) and from the 2004 to present Ice-Tethered Profiler (ITP) instrumentation system (Krishfield et al. 2008). Compared to the 1975 AIDJEX dataset, the ITP dataset is associated with lower sea ice concentration (Fig. 1), has less multiyear sea ice area and volume (Wadhams 2012; Kwok 2018), and is made up of smaller ice floes (Hutchings and Faber 2018) that are both thinner (Kwok and Rothrock 2009; Kwok 2018) and less deformed, with shallower ridges (Wadhams 2012; Hutchings and Faber 2018; Kwok 2018).

Both the ITP and AIDJEX data were collected in the Canada Basin (Fig. 1), where the upper-ocean hydrography evolves seasonally in response to changes in sea ice (McPhee and Smith 1976; Morison and Smith 1981; Lemke and Manley 1984; Jackson et al. 2010; Toole et al. 2010; Peralta-Ferriz and Woodgate 2015), river runoff (Macdonald et al. 1999; Yamamoto-Kawai et al. 2009), and Ekman dynamics in the Beaufort Gyre (Proshutinsky et al. 2009; Carmack et al. 2016; Meneghello et al. 2018). In the spring and summer, freshwater flux from snow and sea ice melt causes the surface mixed layer to freshen and shoal, forming a seasonal halocline. The predominant, clockwise atmospheric circulation (Beaufort high) drives convergent Ekman pumping in the Beaufort Gyre most noticeably in the fall, causing low-salinity surface water to converge and the halocline to deepen within the basin (Reed and Kunkel 1960; Gudkovich 1961; Hunkins and Whitehead 1992; Proshutinsky et al. 2009; Newton et al. 2006; Jackson et al. 2010; McLaughlin and Carmack 2010; Meneghello et al. 2018). In the winter, sea ice formation results in brine rejection, which increases the surface water salinity and causes convectively driven mixed layer deepening that erodes the seasonal halocline.

Comparisons of single representative profiles from ITP and AIDJEX data that were collected in roughly the same location indicate a trend toward fresher surface waters, shallower mixed layers, and a more stably stratified upper ocean (Toole et al. 2010; McPhee 2012), similar to the comparison of AIDJEX and 1997 Surface Heat Budget of the Arctic (SHEBA) data (McPhee et al. 1998). June–September and November–May seasonal averages of hydrographic data across the Arctic during 1979–2012, which did not include ITP or AIDJEX data, confirmed statistically significant ~30-yr trends toward a more stably stratified upper ocean with shallower and fresher mixed layers in the Canada Basin (Peralta-Ferriz and Woodgate 2015). Decadal changes to the surface waters were primarily attributed to increased freshwater input from ice melt, river runoff, and precipitation. This freshwater has collected toward the center of an intensified anticyclonic (convergent) Beaufort Gyre (Macdonald et al. 1999; Proshutinsky et al. 2009; Jackson et al. 2010; McLaughlin and Carmack 2010; Steele et al. 2011; Peralta-Ferriz and Woodgate 2015). However, the seasonality of the freshwater input, the vertical extent of wind-driven mixing, and upper-ocean stratification was not addressed in these previous studies.

In this study, we compare seasonal processes of the upper ocean by focusing on the evolving time series from May to September in the 2006–12 ITP data and 1975 AIDJEX data. This seasonal analysis differs from previous studies that compared two single profiles (Toole et al. 2010; McPhee et al. 1998), two 20-day average profiles (McPhee 2012), or used 4- and 7-month averages (Peralta-Ferriz and Woodgate 2015). We interpret the results using a simple one-dimensional bulk model of seasonal halocline formation that allows for the comparison of the ITP and AIDJEX data in terms of seasonal freshwater input and vertical mixing. The datasets used for this study are presented in section 2, and the one-dimensional model is presented in section 3. In section 4, we present results comparing the ITP and AIDJEX hydrographic data in conjunction with the one-dimensional model metrics. We discuss broad implications of the results for coupled models and mechanisms that could explain changes in the relationship between freshwater input, vertical mixing, and stratification during the two time periods in section 5 and summarize our results in section 6.

2. Data

This study addresses spring-to-summer halocline formation associated with two distinctly different time periods and sea ice

TABLE 1. List of AIDJEX ice camps and ITPs used in the study.

	Time period used
Ice camp	
Blue Fox	10 May–31 Sep 1975
Caribou	14 May–31 Sep 1975
Snowbird	16 May–31 Sep 1975
Big Bear	1 May–31 Sep 1975
ITP	
1	1 May–31 Sep 2006
3	1 May–10 Sep 2006
4	1 May–17 Aug 2007
5	1 May–2 Aug 2007
6	1 May–31 Sep 2007
8	1 May–31 Sep 2008
11	1 May–20 Jul 2009
13	1 May–8 Aug 2008
18	1 May–31 Sep 2008
33	1 May–31 Sep 2010
41	1 May–31 Sep 2011
41	1 May–31 Sep 2012
53	1 May–5 Aug 2012

regimes. To this end, we use observed May–September near-surface salinity profiles from the AIDJEX and ITP programs.

A major component of the AIDJEX program consisted of four occupied, drifting ice camps where oceanographic data were collected for approximately one year between May 1975 and April 1976 (Table 1). Salinity and temperature profiles between depths of 5 and 750 m were measured daily at each camp, with a vertical resolution of 1–2 m, using a Plessey model 9040 conductivity, temperature, depth measurement system, resulting in 1279 vertical profiles. See Maykut and McPhee (1995) for a full description of the data used in this analysis.

The ITP instrument system records temperature and salinity profiles with a vertical resolution of 25 cm throughout the Arctic. The system consists of a series of surface buoys, frozen into drifting ice floes, connected to 800-m-long wires. CTD profilers move up and down the wires collecting data approximately 2–3 times per day. We use quality-controlled data, identified as level 3 in the ITP data archives, which have 1-m vertical resolution and were available for 2004–12 at the time of the analysis. We examine all available level-3 processed data within the Canada Basin, which we define as the region bounded by 72°N, 80°N, 130°W, and 155°W [similar to the region defined by Peralta-Ferriz and Woodgate (2015); dashed lines, Fig. 1]. Further, we select only ITPs that have data starting in May of a given year, similar to the data available from the AIDJEX ice camps. Last, profiles were removed if the shallowest observed value was deeper than 10 m (following Jackson et al. 2010), which helps to account for the fact that ITPs often start sampling too deep to accurately measure the summer mixed layer.

In total, 517 AIDJEX profiles collected in 1975 from four ice camps and 2892 ITP profiles collected between 2006 and 2012 from 12 different ITPs satisfied these criteria (Table 1), with average shallowest measurements of ~6 and ~7 m, respectively. All profiles were linearly interpolated onto a common 1-m vertical grid. Ice thickness measurements are not available for all ITP profiles or AIDJEX ice camps. For both datasets, we therefore assume an ice–ocean interface at 3 m, a climatological multiyear sea ice thickness in the Canada Basin (Perovich and Richter-Menge 2015), and keep the salinity and temperature constant from the shallowest measurements of each profile to $z = -3$ m, with the z axis defined as positive up. We discuss the sensitivity of our results to missing near-surface data in section 5.

To estimate the freshwater input from sea ice melt, we also examine 1979–2018 sea ice volume estimates provided by the Pan-Arctic Ice Ocean Modeling and Assimilation System (PIOMAS; Schweiger et al. 2011). The PIOMAS sea ice volume was regridded to the 25 km Equal-Area Scalable Earth (EASE) grid and averaged over the Canada Basin (bounded by 72°N, 80°N, 130°W, and 155°W, as in the hydrographic data).

To qualitatively compare the sea ice conditions associated with the AIDJEX and ITP datasets, we examine 1975 and 2006–12 sea ice concentrations. Daily 2006–12 sea ice concentration observations are provided by passive microwave satellite data, version 1 (Cavalieri et al. 1996), which combines data from the Defense Meteorological Satellite Program Special Sensor Microwave Imager (DMSP SSM/I, 2006–07) and the Special Sensor Microwave Imager/Sounder (SSMI/S, 2007–12). Sea ice concentration data are collocated to each ITP observation. We note that low sea ice concentration from the passive microwave data can imply either low ice concentration or surface melt ponds (e.g., Kern et al. 2016). Since the AIDJEX data were collected in 1975, before the satellite data were available, we use the Canadian Ice Service digital archive (CISDA) chart data for the western Arctic region to determine the temporal evolution of sea ice concentration during that year in the Canada basin region (Tivy et al. 2011). Gridded datasets for each CISDA chart in June–September 1975 were analyzed to provide a weekly regional mean sea ice concentration.

3. One-dimensional framework

One-dimensional (1D) ice–ocean bulk models are used to provide a framework for interpreting observed seasonal mixed layer evolution (Morison and Smith 1981; Lemke and Manley 1984; Lemke 1987; Toole et al. 2010; Petty et al. 2013; Tsamados et al. 2015; Peralta-Ferriz and Woodgate 2015; Randelhoff et al. 2017). Here, we model seasonal halocline formation starting from a homogeneous winter mixed layer in an idealized system (Fig. 2), building on conceptual models used to estimate freshwater input, vertical mixing, and upper-ocean stratification from hydrographic data in previous studies (Lemke and Manley 1984; Peralta-Ferriz and Woodgate 2015; Randelhoff et al. 2017). The resulting framework provides a suite of diagnostic, upper-ocean parameters to examine the vertical salt budget and its impact on the stratification using the observed seasonal evolution of vertical salinity profiles. This idealized model omits a range of processes,

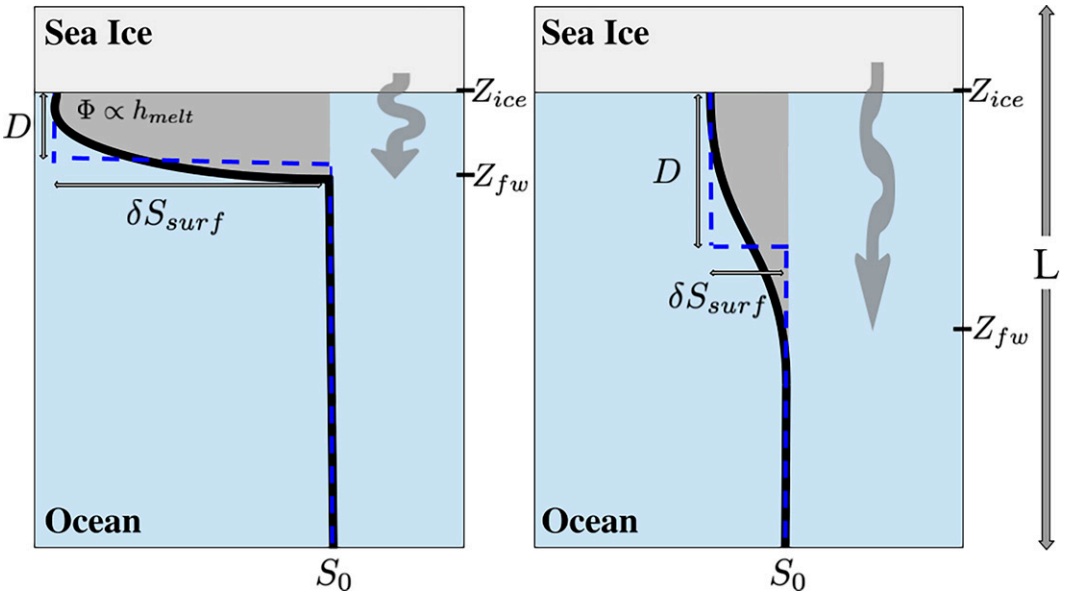

FIG. 2. Schematic of one-dimension ice–ocean model, showing an illustration of the salinity profile resulting from (left) ice melt that is concentrated close to the surface and (right) an example where a similar amount of ice melt is mixed over a larger depth range. Here, L is the depth of the ocean; D, Z_{ice}, and Z_{fw} are negative values that indicate depths; S_0 and δS_{surf} indicate the initial salinity and surface freshening, respectively. Area covered by gray shading is equal to Φ and linearly related to the equivalent sea ice melt (h_{melt}). Vertical and horizontal blue dashed lines indicate D and δS_{surf}, respectively. Gray arrows represent the vertical extent of sea ice meltwater.

including 1) temperature effects on density, which have a less than 1% impact of the surface density in the ITP data (not shown); 2) brine-rejection driven mixing from intermittent freezing, which cannot be resolved from daily observations; 3) tidal currents, which are only expected to impact shelf waters (i.e., shallower than in the Canada Basin); and 4) double diffusion, which mainly impacts the 200–300-m depth range in this region (Timmermans et al. 2008), and a range of processes associated with horizontal advection. The impact of this will be considered in sections 4 and 5.

a. Model equations

We consider a closed, 1D ice–ocean system with an ocean of depth L that only evolves in response to thermodynamic spring–summer sea ice melt and vertical mixing with the following initial conditions ($t = t_0$): a well-mixed ocean, with vertically uniform salinity (S_0) and potential density (ρ_0), and sea ice with constant salinity (S_{ice}) and density (ρ_{ice}).

If meltwater is vertically mixed to some depth Z_{fw}, then the salinity and density below this depth remains fixed at S_0 and ρ_0 [i.e., $S(z) = S_0$ and $\rho(z) = \rho_0$ for $z \le Z_{\text{fw}}$, where z and Z_{fw} are both negative]. The conservation of salt and mass for time $t > t_0$ can then be written as

$$\int_{Z_{\text{fw}}(t)}^{Z_{\text{ice}}} \rho(t,z)S(t,z)dz - \rho_0 S_0\left[Z_{\text{ice}} - Z_{\text{fw}}(t)\right] = \rho_{\text{ice}} S_{\text{ice}} h_{\text{melt}}(t) \tag{1}$$

$$\int_{Z_{\text{fw}}(t)}^{Z_{\text{ice}}} \rho(t,z)dz - \rho_0\left[Z_{\text{ice}} - Z_{\text{fw}}(t)\right] = \rho_{\text{ice}} h_{\text{melt}}(t), \tag{2}$$

where t is a seasonally evolving time variable; Z_{ice} is the ice draft; h_{melt} is the change in sea ice thickness from melt; $\rho(t, z)$ and $S(t, z)$ are the ocean potential density and salinity, respectively. The above expressions, therefore, represent the change in mass and salt in the ocean (left-hand side) in response to sea ice melt (right-hand side). These equations can be algebraically combined to estimate the sea ice melt necessary to explain the transition from the initial, well-mixed ocean (S_0, ρ_0) to the subsequent ocean profile that includes vertically mixed meltwater [$S(t, z)$, $\rho(t, z)$] at any time $t > t_0$:

$$h_{\text{melt}}(t) = \int_{Z_{\text{fw}}(t)}^{Z_{\text{ice}}} \frac{\rho(t,z)\left[S(t,z) - S_0\right]}{\rho_{\text{ice}}(S_{\text{ice}} - S_0)} dz, \tag{3}$$

where h_{melt} represents a time-evolving integral measure of seawater dilution by cumulative surface freshwater input from sea ice melt. This approach is similar to an approach used in previous studies that estimated sea ice melt from mixed layer salinity evolution (Lemke and Manley 1984; Peralta-Ferriz and Woodgate 2015), but here the depth range is set by Z_{fw} and Z_{ice} rather than a mixed layer depth criterion. That is, we estimate the freshwater input from sea ice melt over a well-defined volume, which avoids errors that can arise when using an arbitrary reference salinity (Schauer and Losch 2019; Rosenblum et al. 2021).

The term h_{melt} is linearly related to the vertically integrated change in salinity relative to S_0:

$$\Phi(t) = \int_{Z_{\text{fw}}(t)}^{Z_{\text{ice}}} \left[S_0 - S(t,z)\right]dz, \tag{4}$$

which also provides a bulk estimate of the cumulative amount of freshwater input at any time $t > t_0$. We note that Φ is closely related to the "salt deficit" or "buoyancy deficit" as defined by Martinson (1990), Martinson and Iannuzzi (1998), and Randelhoff et al. (2017).

Different salinity profiles are possible in response to the same amount of ice melt, depending on how the meltwater is vertically spread or mixed through the water column (Fig. 2). For example, if the meltwater were concentrated close to the surface (less vertical mixing, shallow Z_{fw}), this would result in more surface freshening and a more stably stratified water column (Fig. 2; left side). Alternatively, if the meltwater were spread over a larger depth range (more vertical mixing, deep Z_{fw}), this would result in less surface freshening and a less stably stratified water column (Fig. 2; right side).

To quantify this effect, we will consider two bulk metrics of stratification. First, we define the surface freshening at any time $t > t_0$ as the surface salinity anomaly relative to the initial condition:

$$\delta S_{surf}(t) = S(t, Z_{ice}) - S_0. \tag{5}$$

Second, we define the stratification that occurs in response to sea ice melt at any time $t > t_0$ as the vertical derivative of salinity averaged over depth Z_{fw}:

$$S_z(t) = \frac{1}{Z_{fw}(t) - Z_{ice}} \int_{Z_{fw}(t)}^{Z_{ice}} \frac{dS(t,z)}{dz} dz. \tag{6}$$

b. Separating freshwater input and vertical mixing

We seek representations of δS_{surf} and S_z to directly compare the 1975 AIDJEX data and 2006–12 ITP data in terms of changes to 1) the seasonal freshwater input and 2) vertical mixing. That is, for any time $t > t_0$, we seek:

$$\Delta[\delta S_{surf}(t)] = f[\Delta\Phi(t), \Delta D(t)] \tag{7}$$

$$\Delta S_z(t) = f[\Delta\Phi(t), \Delta D(t)]. \tag{8}$$

Here, Δ indicates the difference between ITP and AIDJEX data:

$$\Delta X = X_{ITP} - X_{AJX}, \tag{9}$$

where ITP indicates that the value is derived from ITP data and AJX indicates that the value is derived from AIDJEX data.

Parameter D is a bulk indicator of the vertical mixing, where we define larger and smaller mixing as mixing that leads to a deeper or shallower seasonal halocline. We choose the equivalent mixed layer depth, an integral quantity that is closely related to the vertical extent of wind-driven mixing (similar to Randelhoff et al. 2017):

$$D(t) = \frac{\Phi(t)}{\delta S_{surf}(t)}, \tag{10}$$

where $D + Z_{ice}$ indicates the depth of the halocline if the meltwater were completely mixed (i.e., if the salinity were homogenized), implying that the salinity profile would have a 2-layer form and that $D + Z_{ice} = Z_{fw}$:

$$S_{bulk}(t,z) = \begin{cases} S_0 + \Phi(t)/D(t) & D(t) + Z_{ice} \le z \le Z_{ice} \\ S_0 & z < D(t) + Z_{ice} \end{cases} \tag{11}$$

(see Fig. 2 for an illustration of this 2-layer profile).

The surface freshening (δS_{surf}) and stratification (S_z) associated with this 2-layer system for any time $t \ge t_0$ is

$$\delta S_{surf}(t) = \frac{\Phi(t)}{D(t)} \quad \text{and} \quad S_z(t) = \frac{\Phi(t)}{D(t)^2}, \tag{12}$$

respectively, following Eqs. (5), (6), and (11). The surface freshening δS_{surf}, therefore, indicates the salt content changes within the mixed layer D.

Two factors determine δS_{surf} and S_z: 1) the amount of freshwater input (related to Φ and h_{melt}) and 2) the concentration or dilution of that freshwater toward or away from the surface by vertical mixing (related to D). We can, therefore, estimate how each factor contributes to $\Delta(\delta S_{surf})$ and ΔS_z [as in Eqs. (7) and (8)] by writing δS_{surf} and S_z derived from 2006–12 ITP data in terms of the changes relative to the 1975 AIDJEX data:

$$\delta S_{surf,ITP}(t) = \frac{\Phi_{AJX}(t) + \Delta\Phi(t)}{D_{AJX}(t) + \Delta D(t)}, \tag{13}$$

$$S_{z,ITP}(t) = \frac{\Phi_{AJX}(t) + \Delta\Phi(t)}{[D_{AJX}(t) + \Delta D(t)]^2}. \tag{14}$$

The difference between δS_{surf} in 1975 and 2006–12 [$\Delta(\delta S_{surf})$] can then be rewritten algebraically to isolate the relative contributions of $\Delta\Phi$ and ΔD on $\Delta(\delta S_{surf})$:

$$\Delta[\delta S_{surf}(t)] = \underbrace{\frac{\Delta\Phi(t)}{D_{AJX}(t)}}_{\substack{\text{changes to} \\ \text{freswater input}}} - \underbrace{\frac{\Phi_{AJX}(t)\Delta D(t)}{D_{AJX}(t)D_{ITP}(t)}}_{\substack{\text{changes to} \\ \text{vertical mixing}}} - \underbrace{\frac{\Delta\Phi(t)\Delta D(t)}{D_{AJX}(t)D_{ITP}(t)}}_{\text{correlated term}}. \tag{15}$$

Similarly, the difference between S_z in 1975 and 2006–12 (ΔS_z) can be written as

$$\Delta S_z(t) = \underbrace{\frac{\Delta\Phi(t)}{D_{AJX}(t)^2}}_{\substack{\text{changes to} \\ \text{freshwater input}}} \underbrace{- \Phi_{AJX}(t)\Delta D(t)\frac{D_{AJX}(t) + D_{ITP}(t)}{D_{AJX}^2(t)D_{ITP}^2(t)}}_{\substack{\text{changes to} \\ \text{vertical mixing}}} \underbrace{- \Delta\Phi(t)\Delta D(t)\frac{D_{AJX}(t) + D_{ITP}(t)}{D_{AJX}^2(t)D_E^2(t)}}_{\text{correlated term}} \tag{16}$$

(see online supplemental material for full derivation).

The three terms on the right-hand sides of (15) and (16) are estimates of the decadal changes to the stratification associated with 1) changes related to only freshening (freshwater input; $\Delta\Phi$, Δh_{melt}), holding the vertical mixing to AIDJEX values (D_{AJX}); 2) changes related to only mixed layer shoaling

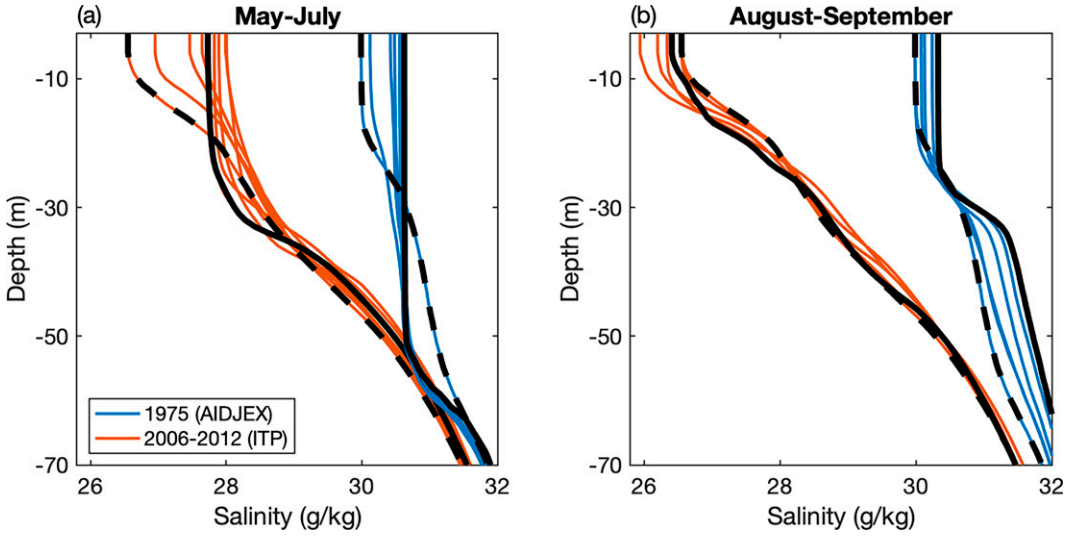

FIG. 3. 10-day mean profiles during (a) May–July and (b) August–September in 1975 (blue) and 2006–12 (red). Solid black lines indicate 10-day mean profiles from (a) the beginning of May and (b) the end of September. Dashed lines indicate common 10-day mean profile that marks the end of July and the beginning of August, (30 Jul–8 Aug) and are the same in (a) and (b). Note that in May, when the freshwater input from sea ice melt is small, changes to the average near-surface salinity are small compared to the spatial and interannual variability (Fig. S1 in the online supplemental material).

(vertical mixing; ΔD), holding the amount of freshwater input equal to AIDJEX values (Φ_{AJX}); and 3) the contribution from the correlation between $\Delta\Phi$ and ΔD.

4. Results

The observations indicate that the surface is ~2–4 g kg^{-1} fresher in 2006–12 relative to 1975, yet both time periods have a similar seasonal evolution (Fig. 3). At the beginning of May, both datasets indicate mixed layers that are relatively deep (thick black lines, Fig. 3a). As spring progresses, the surface freshens and the seasonal halocline forms (dashed black lines, Figs. 3a,b). Toward the end of summer, sea ice forms, the surface becomes progressively saltier, and the mixed layer deepens, eroding the seasonal halocline (cf. dashed and thick black lines, Fig. 3b). Compared to 1975, 2006–12 appears to have more seasonal freshwater stored closer to the surface, resulting in more seasonal surface freshening and a more stably stratified upper ocean for a longer time period. Qualitatively, this is consistent with the previous studies described in section 1.

To compare the seasonal evolution of the upper ocean during 1975 and 2006–12 using the 1D framework, we set S_0 equal to the May-average surface salinity [$S(Z_{ice})$] measured by the same ITP or AIDJEX ice camp during the same year. That is, we examine the seasonal freshwater input (Φ, h_{melt}), vertical mixing (Z_{fw}, D), and the surface freshening (δS_{surf}) relative to the May average, which marks the beginning of the melt season measured by a given ITP or AIDJEX ice camp. We present results based on alternative values of S_0 in the supplemental material. All other constants are given in Table 2.

Figure 4 shows an example of how various quantities presented in section 3 are computed for a single profile using observations from one AIDJEX ice camp (Fig. 4, left side) and one ITP (Fig. 4, right side). The freshwater input, indicated by h_{melt} and Φ, reflects any process that drives changes to the integrated upper-ocean salinity, including sea ice melt, river runoff, precipitation, or advection, although previous studies have demonstrated that the majority of the seasonal freshwater input during the melt season is derived from sea ice melt (e.g., Lemke and Manley 1984; Peralta-Ferriz and Woodgate 2015). Vertical mixing, indicated by Z_{fw} and D, reflects any process that vertically spreads or distributes that freshwater, including wind-driven mixing, and possibly brine-rejection from intermittent freezing, double diffusion, or tidal currents.

a. Validation

To test the validity of our approach, we compare the cumulative seasonal freshwater input in terms of the equivalent ice

TABLE 2. List of constants and variable names.

Name	Description	Value/equation
Z_{ice}	Ice–ocean interface	3 m
β	Haline contraction coefficient	0.81 kg^2 m^{-3} g^{-1}
ρ_{ice}	Sea ice density	900 kg m^{-3}
S_{ice}	Sea ice salinity	5 g kg^{-1}
δS_{surf}	Seasonal surface freshening	Eq. (15)
S_z	Stratification	Eqs. (6), (12)
$S_{z,bulk}$	As in S_z but for 2-layer system	Eq. (12)
h_{melt}	Freshwater input in terms of ice melt	Eq. (3)
Φ	Measure of freshwater input	Eq. (4)
Z_{fw}	Penetration depth of freshwater input	Eq. (3)
D	Equivalent mixed layer depth	Eq. (10)

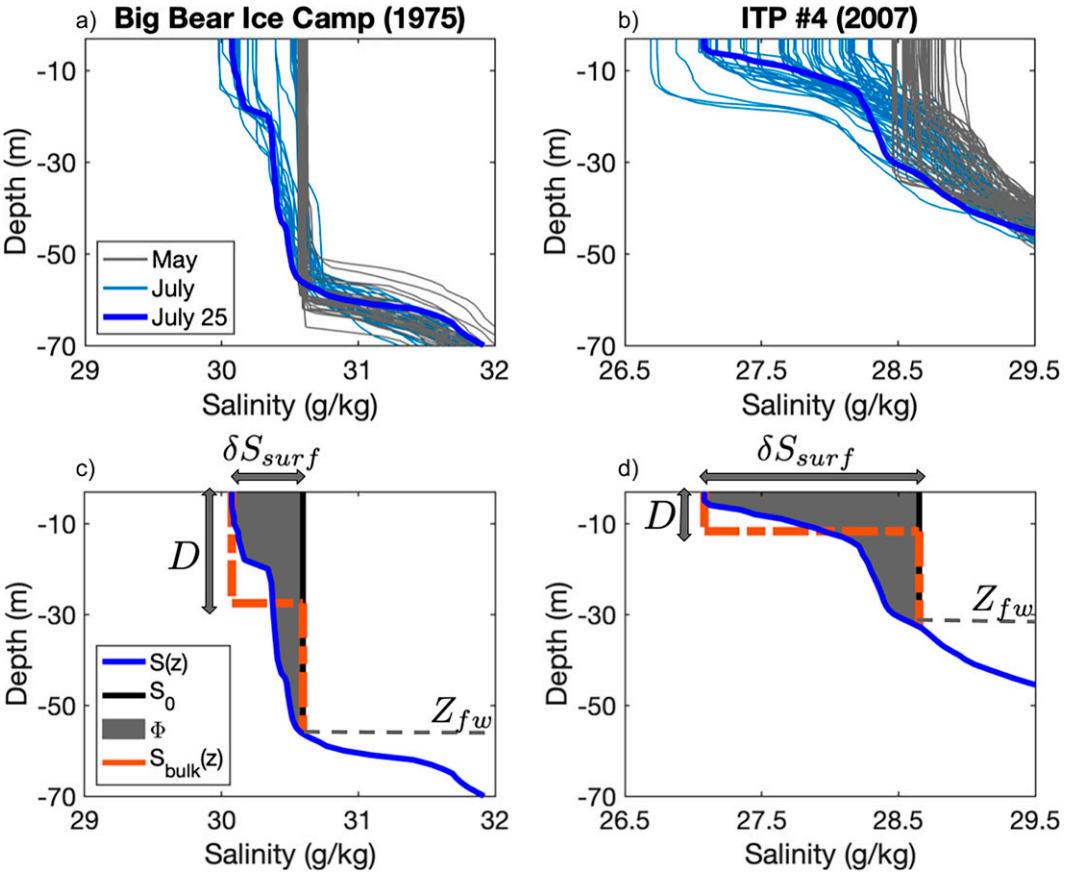

FIG. 4. Observed salinity profiles using data from (left) AIDJEX Big Bear ice camp in 1975 and (right) ITP 4 in 2007 to illustrate the methods used to estimate metrics derived in section 3. (a),(b) All observed salinity profiles measured during the month of May (gray lines) and July (blue lines), with 25 Jul highlighted in dark blue [$S(z)$]. (c),(d) Black line indicates May average surface salinity (S_0), area covered by gray shading is the same as Φ associated with the observed 25 Jul profile. The associated 2-layer salinity profile [red dashed lines, $S_{\text{bulk}}(z)$], which give the surface freshening δS_{surf} and equivalent mixed layer depth D, is shown in red. Blue lines are the same in (a) and (c) and (b) and (d).

melt (h_{melt}), derived from hydrographic data, to the effective ice thickness change relative to May of each year between 1979 and 2018 using PIOMAS. We compute h_{melt} associated with each profile in 1975 and 2006–12. The seasonal evolution of h_{melt} and the monthly ice thickness relative to May are shown in Fig. 5. Both estimates indicate cumulative sea ice melt through August. In 1975, h_{melt} begins to decrease in early September in response to sea ice formation and entrainment. In 2006–12, h_{melt} continues to moderately increase through September in response to a later freeze up (Fig. 5a). We find similar results using different definitions of S_0 (see Fig. S2 in the online supplemental material).

We find good agreement between the PIOMAS seasonal ice thickness changes and the estimated seasonal freshwater input, represented as equivalent meters of ice melt using oceanographic observations during summer, consistent with previous studies. By the end of August, we find $h_{\text{melt}} \sim 0.5$–1 m in 1975 and $h_{\text{melt}} \sim 1$–2 m in 2006–12, consistent with estimated sea ice melt during similar time periods using hydrographic data (Lemke and Manley 1984; Peralta-Ferriz and Woodgate 2015) and ice mass balance buoys (e.g., Perovich and Richter-Menge 2015). The consistency of these findings provides indirect evidence that h_{melt} is a reasonable estimate of the seasonal freshwater input. We note that in June, some data points indicate a negative h_{melt}. For the remainder of the analysis, we only consider profiles with positive values of h_{melt}.

Using each observed profile, we compare the stratification [S_z; Eq. (6)] to the associated 2-layer estimate [Eq. (12)]. The seasonal evolution of each of these values in the 1975 AIDJEX and 2006–12 ITP datasets is shown in Fig. 6. We find a clear agreement between the observations and the 2-layer estimates. First, both values indicate that the seasonal halocline forms in late June of 1975 and 2006–12, but is more stably stratified for a longer period of time in 2006–12. Second, both values are up to 5 times larger in 2006–12 relative to 1975. Toward the end of the melt season, more freshwater is stored below the mixed layer, causing the 2-layer formalism to overestimate S_z. Despite these differences, overall, we find that the 2-layer simplification captures the majority of the key

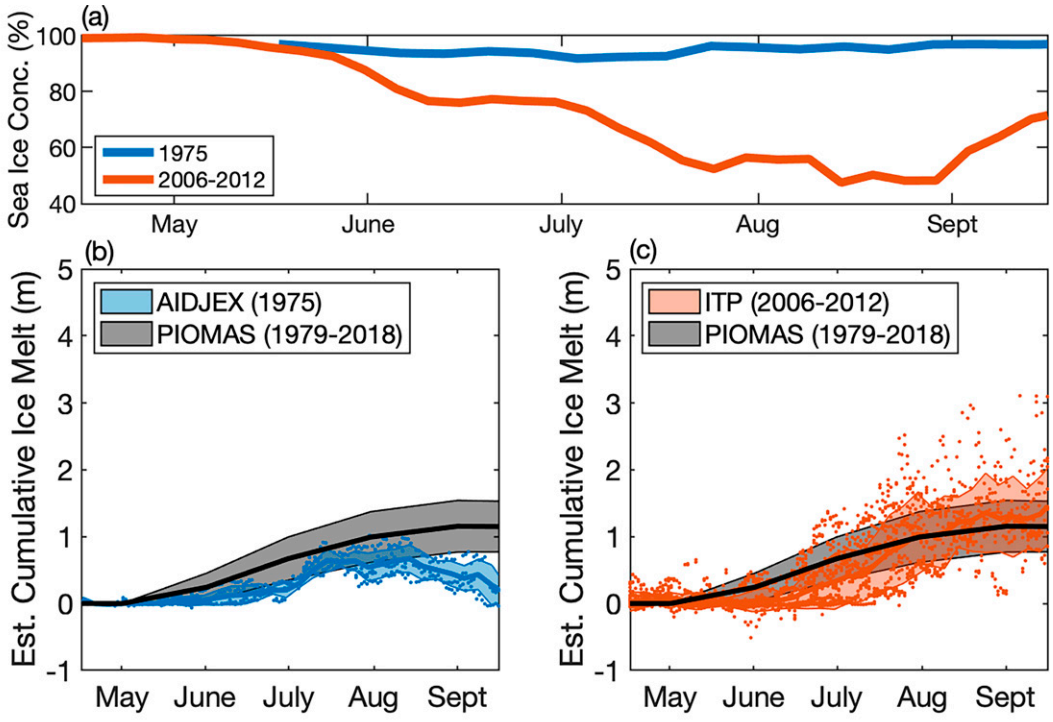

FIG. 5. (a) Sea ice concentration and (b),(c) estimated freshwater input in terms of cumulative sea ice thickness changes (h_{melt}) in 1975 (blue), 2006–12 (red). PIOMAS data provide a climatological monthly effective sea ice thickness change relative to May of each year between 1979 and 2018 (black). Blue and red lines indicate 5-day mean, black lines indicate monthly mean, and shadings indicate one standard deviation.

features necessary to explain the differences between the upper-ocean seasonal evolution in 1975 and 2006–12.

The equivalent mixed layer depth (D) and the associated surface freshening (δS_{surf}) in 1975 and 2006–12 are shown in Fig. 7. These metrics indicate a number of differences between the ITP and AIDJEX datasets that are consistent with previously documented decadal trends in the Canada Basin. Specifically, Peralta-Ferriz and Woodgate (2015) found statistically significant trends of mixed layer freshening (0.11 psu yr^{-1}) and mixed layer shoaling (0.33 m yr^{-1}) during June–September in regions of the Canada Basin with high sea ice concentration (>15%). These rates of change would imply an average change of 3.7 psu and 11.2 m over 34 years, similar to the 3.1 g kg^{-1} and 14.5 m difference in the surface salinity

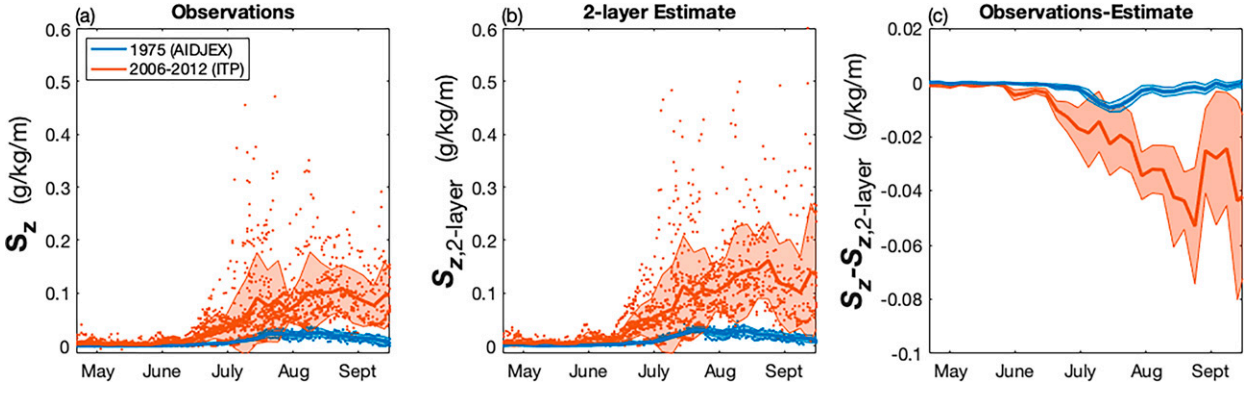

FIG. 6. Validation of the 2-layer approximation of the salinity profile by comparing (a) the stratification [S_z; Eq. (6)] to (b) the associated 2-layer estimate [center; Eq. (12)], and (c) their difference in 1975 (blue) and 2006–12 (red). The stratification S_z is computed for each observed profile. Lines indicate 5-day means, and shading indicates one standard deviation (left and center panels) or standard error (right panels).

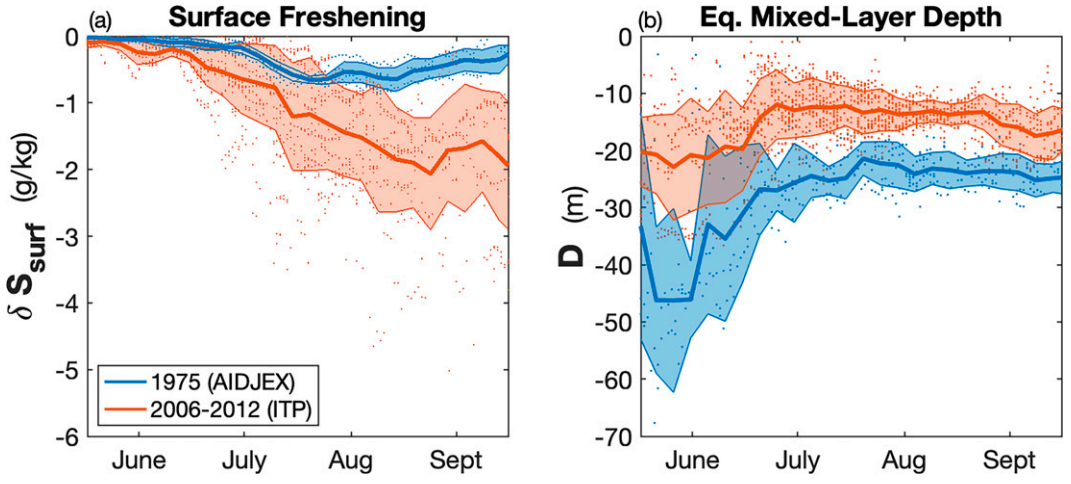

FIG. 7. (a) Surface freshening (δS_{surf}) and (b) equivalent mixed layer depth (D) in 1975 (blue) and 2006–12 (red). The δS_{surf} and D are computed for each observed profile. Lines indicate 5-day means, and shading indicates one standard deviation.

($\delta S_{surf} + S_0$) and the equivalent mixed layer depth (D) between the 1975 AIDJEX data and the 2006–12 ITP data over the same months. Overall, these findings suggest that a comparison of the ITP and AIDJEX datasets, in conjunction with the one-dimensional framework presented in section 3, yields results that are consistent with Peralta-Ferriz and Woodgate (2015) using seasonal averages.

b. 1975 versus 2006–12

The relationship between 1D bulk estimates of freshwater input from ice melt and other freshwater sources [h_{melt}; Eq. (3)], vertical mixing [D; Eq. (10)], and upper-ocean stratification [δS_{surf}, S_z; Eq. (12)] is shown in Fig. 8, using every June–September salinity profile in 1975 and 2006–12. During each time period, we find that the parameters exhibit relationships that are qualitatively consistent with a 1D system: Surface fluxes that result in a more buoyant surface layer cause a more stable stratification that inhibits vertical mixing (Turner 1967; Kraus and Turner 1967; Lemke and Manley 1984; Lemke 1987). That is, profiles with more freshwater input (larger h_{melt}) are associated with less vertical mixing (smaller $|D|$, where $|\cdot|$ indicates the absolute value) and a more stably stratified upper ocean (large $|\delta S_{surf}|$, S_z).

Considering differences between 1975 and 2006–12, we find that there are more profiles in 2006–12 with large values of h_{melt} and hence small values of $|D|$ and large values of $|\delta S_{surf}|$ and S_z, as in a 1D system. However, we also consistently find profiles with the same amount of freshwater (h_{melt}) in both time periods but with the freshwater concentrated closer to the surface (smaller $|D|$) in 2006–12 relative to 1975 (Fig. 8a). These differences in $|D|$ are also associated with a more stable stratification (large $|\delta S_{surf}|$, S_z; Figs. 8b,c). That is, there are two separate factors causing the more stable stratification in 2006–12 relative to 1975: 1) more freshwater input (larger h_{melt}), which mainly occurs in August and September, and 2) less vertical mixing (smaller $|D|$), which mainly occurs in June and July (Fig. 8, compare top and bottom panels).

We find similar results when examining the relationship between $\Delta(\delta S_{surf})$, ΔS_z, and Δh_{melt} during each 5-day period (Fig. 9); 5-day periods with similar levels of freshwater input in 1975 and 2006–12 ($\Delta h_{melt} \sim 0$) have different stratification [$|\Delta(\delta S_{surf})| > 0$, $\Delta S_z > 0$] from June until mid-August. The largest difference between the two time periods occurs from mid-August through September, coinciding with the largest values of Δh_{melt}.

We can use the 1D framework (section 3b) to estimate the relative importance of each of these factors in setting the more stable stratification in 2006–12 relative to 1975. Figures 10b and 10c show the 5-day average bulk estimates of the upper-ocean stratification (δS_{surf}, S_z) in 1975 (blue line) and 2006–12 (red line). For each 5-day period, we compute the difference between 1975 and 2006–12 [$\Delta(\delta S_{surf})$, ΔS_z] in terms of 1) the larger freshwater input alone (yellow region; $\propto \Delta h_{melt}$, $\Delta\Phi$), 2) the concentration of the freshwater closer to the surface alone (purple region; $\propto \Delta D$), and 3) the contribution from the correlation between the two factors (green region; $\propto h_{melt}\Delta D$, $\Delta\Phi\Delta D$) using Eqs. (15) and (16). The yellow region provides a rough estimate of the change in stratification that would occur if the relatively large amount of freshwater input indicated by 2006–12 ITP data is stored within the relatively deep mixed layer measured by 1975 AIDJEX data [i.e., if $\Delta D = 0$ in Eqs. (15) and (16)]. Similarly, the purple region provides a rough estimate of the change in stratification that would occur if the relatively small amount of freshwater input indicated by 1975 AIDJEX data is stored within the relatively shallow mixed layer measured by 2006–12 ITP data [i.e., if $\Delta\Phi = 0$ in Eqs. (15) and (16)].

Overall, the changes to the vertical mixing (ΔD), the freshwater input ($\Delta\Phi$), and the contribution from the correlation between the two terms ($\Delta\Phi\Delta D$) have similar roles in explaining the larger magnitudes of $|\Delta(\delta S_{surf})|$ and S_z in 2006–12 relative to 1975. This implies that the concentration of freshwater closer to the surface in recent years has a similar impact on upper-ocean stratification to that caused by a larger amount

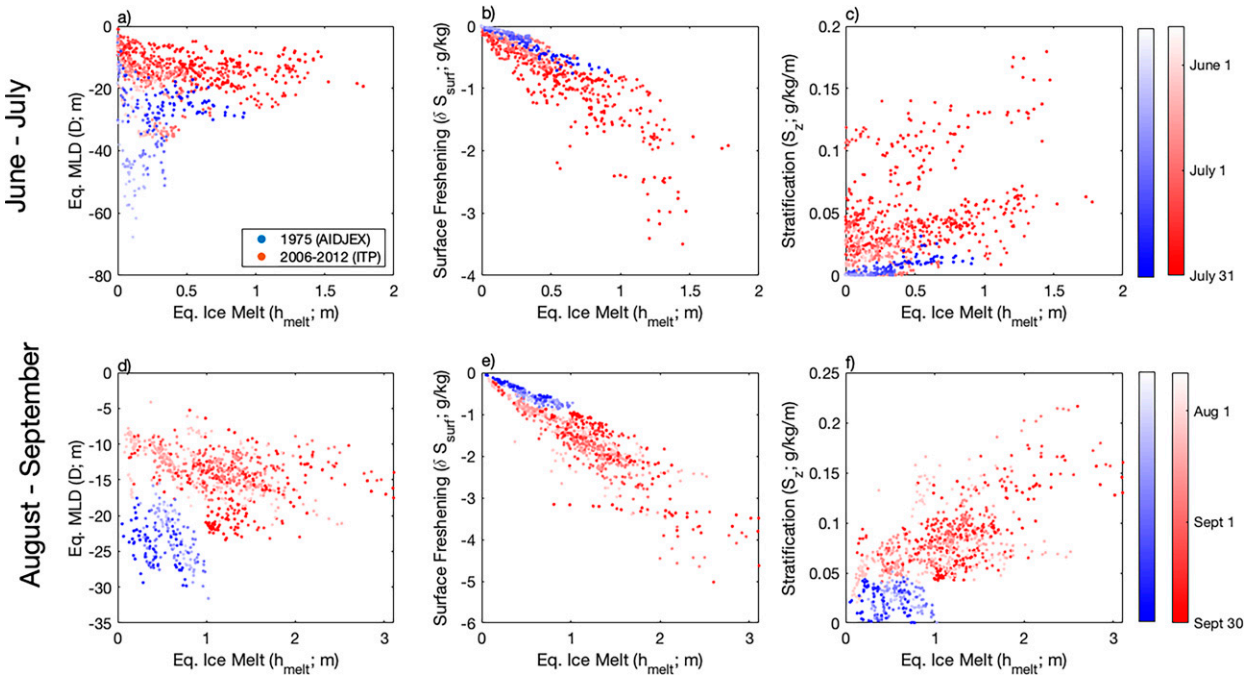

FIG. 8. Relationships between equivalent sea ice melt (h_{melt}) and (a),(d) equivalent mixed layer depth (D), (b),(e) surface freshening (δS_{surf}), and (c),(f) upper-ocean stratification (S_z) using vertical salinity profiles in 1975 (blue) and 2006–12 (red) during (top) June–July and (bottom) August–September. Shadings indicate date of measurement.

of seasonal freshwater input. The seasonality of the two factors confirms our findings from Fig. 9: the concentration of freshwater closer to the surface (purple region) is mainly important in June–August, while the larger amount of freshwater input and the correlated term (yellow and green regions) are mainly important in August–September. This result is also consistent with the largest differences in h_{melt} between the two time periods occurring toward the end of the melt season (Fig. 10a).

5. Discussion

Coupled ice–ocean models and global climate models are used extensively to understand current climate change and to predict future changes, but tend to simulate an upper-ocean stratification in the Canada Basin that is weaker than observed (Holloway et al. 2007; Ilıcak et al. 2016; Nguyen et al. 2009; Zhang and Steele 2007; Jin et al. 2012; Barthélemy et al. 2015; Sidorenko et al. 2018; Rosenblum et al. 2021). In a climate model, Φ is directly related to the freshwater flux at the surface due to sea ice melt, river runoff, and precipitation, while D is closely related to simulated ocean mixed layer dynamics (Rosenblum et al. 2021). In Fig. 10, the yellow region provides a rough estimate of the more stable stratification that would occur in a model that accurately simulated decadal changes to freshwater fluxes with unchanged mixed layer dynamics. The purple region provides a rough estimate of the more stable stratification that would occur in a model that accurately simulated decadal changes to mixed layer dynamics without simulating changes to freshwater fluxes. Climate models that do not simulate the decadal trend toward a shallower mixed layer in the Canada Basin (Rosenblum et al. 2021), therefore, do not include the contributions toward a more stratified upper ocean that are quantified by the purple and green regions of Fig. 10.

What mechanisms caused shallower mixed layers and stronger stratification in 2006–12 in response to the same amount of freshwater input as in 1975 (associated with the purple regions of Fig. 10)? One possibility is that lateral processes are more prominent under the more mobile ice cover in recent years and cause complicated relationships between freshwater input, vertical mixing, and stratification (Randelhoff et al. 2017; Meneghello et al. 2021) or establish fronts that act to limit the effects of wind-driven vertical mixing via submesoscale instabilities (Timmermans and Winsor 2013). A second possibility is that wind-driven momentum transfer below sea ice has decreased in response to changing sea ice conditions, which can occur in regions that transitioned from multiyear to first-year ice. Specifically, modeling studies suggest that the wind-driven momentum transfer can sometimes decrease in response to the loss of ice keels and reduced sea ice roughness rather than increase in response to enhanced sea ice motion (McPhee 2012; Martin et al. 2014, 2016; Tsamados et al. 2014). A third possibility is that the shallower and more stably stratified winter halocline in 2006–12 inhibited mixed layer deepening to the levels seen in 1975 (Fig. 3; Toole et al. 2010; Peralta-Ferriz and Woodgate 2015). Each of these mechanisms would create a positive feedback scenario in which the same amount of meltwater is concentrated closer to the surface toward the beginning of spring, setting up a more stable

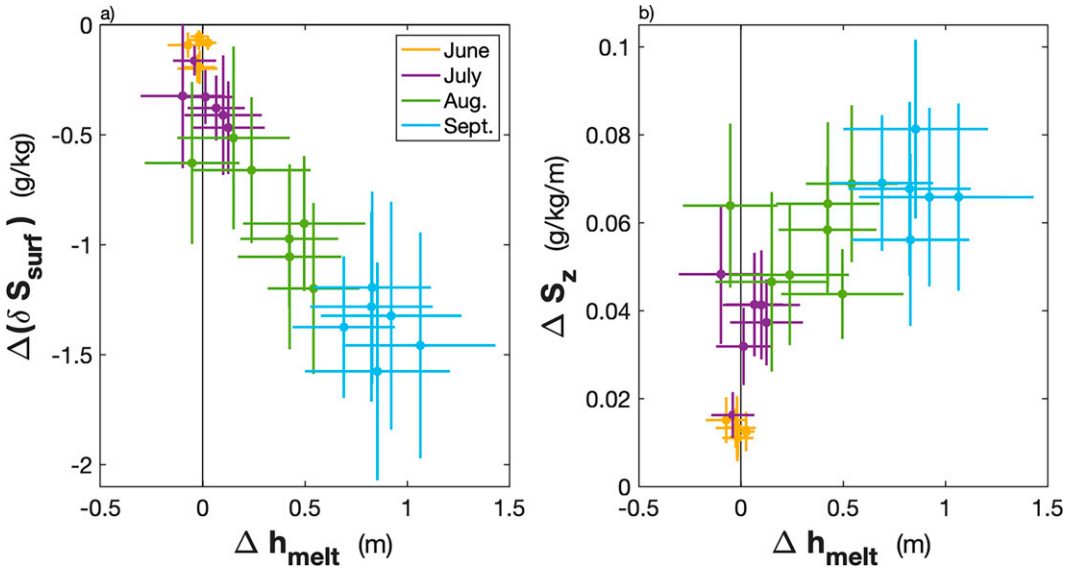

FIG. 9. Five-day average differences between 1975 and 2006–12 using the difference between equivalent ice melt (Δh_{melt}), the surface freshening [$\Delta(\delta S_{surf})$], and stratification (ΔS_z) during the two time periods. Colors indicate month, and lines indicate one standard error.

seasonal halocline that further inhibits vertical mixing of meltwater and further stabilizes the seasonal halocline.

Another possibility is that changes to the sea ice conditions impact melt-pond drainage, which is associated with halocline formation in early summer (Gallaher et al. 2016). Unfortunately, both the ITPs and AIDJEX measurements begin at an average of ~6–7-m depth and, therefore, do not capture important variations to the freshwater content near the surface. This surface data gap can cause mixed layer depths to be biased too deep (Toole et al. 2010), can cause the timing of the mixed layer shoaling to be biased several weeks too late (Gallaher et al. 2017), and can cause uncertainties in the seasonal freshwater storage. Considering results from Proshutinsky et al. (2009), we estimate that this error could cause h_{melt} to be underestimated by approximately 0.2 m during the summer months (see supplemental material for details). More uncertainties arise because we lack measurements of the sea ice draft (Z_{ice}) for the vertical bounds of our calculations. For example, we find that ±1 m changes to Z_{ice} result in approximately ±0.1 m of equivalent ice melt by the end of the melt season.

Overall, the cause of the shallower vertical mixing in recent years remains an open question but one that may be essential for accurately simulating decadal changes to upper-ocean stratification in climate models (Rosenblum et al. 2021). A clear answer to this question will require shallow, near-ice hydrographic or sea ice mass balance measurements in tandem with models to disentangle the sensitivity of vertical mixing to lateral processes, ice–ocean momentum exchange, and premelt conditions.

6. Summary

The rapid and continuing change of summer sea ice cover in the Canada Basin has led to a fresher and more stratified upper ocean that has been primarily attributed to more freshwater input from sea ice melt, river runoff, and Ekman convergence of fresh surface waters within the Beaufort Gyre (e.g., McPhee et al. 1998; Macdonald et al. 1999; Yamamoto-Kawai et al. 2009; Jackson et al. 2010; McLaughlin and Carmack 2010; Steele et al. 2011; Peralta-Ferriz and

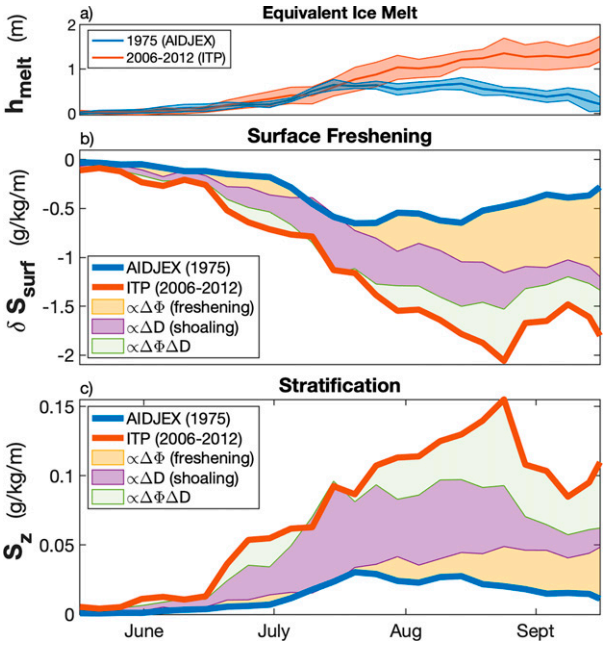

FIG. 10. Five-day mean (a) equivalent ice melt (h_{melt}), (b) surface freshening using the 2-layer estimate (ΔS_{surf}), and (c) stratification using the 2-layer estimate (S_z) in 1975 (blue) and 2006–12 (red). In (b) and (c), colors are associated with three terms that contribute to the difference between 1975 and 2006–12 [$\Delta(\delta S_{surf})$, ΔS_z].

Woodgate 2015; Carmack et al. 2015). The results presented here indicate that decadal changes to ice–ocean dynamics have a similar impact on the changing seasonal halocline as changes to the freshwater input.

We compared the seasonal evolution of the upper ocean salinity below sea ice in 1975 and 2006–12, using data collected from the AIDJEX ice camps and ITPs (Fig. 1; section 2). We interpret differences between the two time periods using a one-dimensional bulk model that allows for the separation of changes in terms of seasonal freshwater input and vertical mixing (Fig. 2; section 3). While upper-ocean dynamics are significantly influenced by spatial and year-to-year variability (Fig. 1; e.g., Yamamoto-Kawai et al. 2009; Peralta-Ferriz and Woodgate 2015; Perovich and Richter-Menge 2015; Proshutinsky et al. 2019; Cole and Stadler 2019), we find that differences between the ITP and AIDJEX datasets yield results that are consistent with decadal trends in the Canada Basin reported by previous studies (Peralta-Ferriz and Woodgate 2015; section 4a).

By examining the relationships between bulk estimates of the freshwater input (h_{melt}), vertical mixing (D), and stratification (δS_{surf}, S_z), we found that two separate factors have a similar impact on creating the stronger stratification in 2006–12 when compared with 1975: larger freshwater input and less vertical mixing (Figs. 8–10). These results stem from the finding that profiles with the same freshwater input are often associated with less vertical mixing and a more stratified upper ocean in 2006–12 relative to 1975, particularly in June–July (Fig. 8). In these cases, the stronger stratification in 2006–12 relative to 1975 appears to be unrelated to seasonal freshwater surface fluxes. These results indicate that ice–ocean dynamics, rather than freshwater input alone, play a crucial role in explaining decadal changes to the seasonal halocline in the Canada Basin.

Acknowledgments. ER was supported by the National Sciences and Engineering Research Council of Canada (NSERC) PDF award, the Chateaubriand Fellowship of the Office for Science and Technology of the Embassy of France in the United States, and the U.S. National Science Foundation (NSF) Graduate Research Fellowship. ER and JS were supported by the NSERC Canada-150 Chair (G00321321). STG was supported by the U.S. NSF (Awards PLR-1425989 and OPP-1936222) and by the U.S. Department of Energy (DOE) (Award DE-SC0020073). This work is a contribution to the NSERC – Discovery Grant and the NSF Office of Polar Program Grant 1504023 awarded to LBT. RG was supported by the NSERC Canada Discovery Grant program. RF acknowledges funding from NSERC Canada through a CGS-D award and the U.S. DOE (Grant DE-SC001940). RF was supported by the NOAA Climate and Global Change Postdoctoral Fellowship Program, administered by UCAR's Cooperative Program for the Advancement of Earth System Sciences, under Award NA18NWS4620043B. The authors thank Sheldon Bacon, Ursula Schauer, and one anonymous reviewer for helpful comments and suggestions.

Data availability statement. The AIDJEX data used in this study can be found at http://lwbin-datahub.ad.umanitoba.ca/dataset/aidjex. The Ice-Tethered Profiler data were collected and made available by the Ice-Tethered Profiler Program based at the Woods Hole Oceanographic Institution (http://www.whoi.edu/itp). All sea ice concentration data created or used during this study are openly available from the NASA National Snow and Ice Data Center Distributed Active Archive Center at https://doi.org/10.5067/8GQ8LZQVL0VL as cited in Cavalieri et al. (1996).

REFERENCES

Barthélemy, A., T. Fichefet, H. Goosse, and G. Madec, 2015: Modeling the interplay between sea ice formation and the oceanic mixed layer: Limitations of simple brine rejection parameterizations. *Ocean Modell.*, **86**, 141–152, https://doi.org/10.1016/j.ocemod.2014.12.009.

Brown, K. A., J. M. Holding, and E. C. Carmack, 2020: Understanding regional and seasonal variability is key to gaining a pan-Arctic perspective on Arctic Ocean freshening. *Front. Mar. Sci.*, **7**, 606, https://doi.org/10.3389/fmars.2020.00606.

Carmack, E. C., and Coauthors, 2015: Towards quantifying the increasing role of oceanic heat in sea ice loss in the new Arctic. *Bull. Amer. Meteor. Soc.*, **96**, 2079–2105, https://doi.org/10.1175/BAMS-D-13-00177.1.

——, and Coauthors, 2016: Freshwater and its role in the Arctic Marine System: Sources, disposition, storage, export, and physical and biogeochemical consequences in the Arctic and global oceans. *J. Geophys. Res. Biogeosci.*, **121**, 675–717, https://doi.org/10.1002/2015JG003140.

Cavalieri, D., C. L. Parkinson, P. Gloersen, and H. J. Zwally, 1996: Sea Ice Concentrations from Nimbus-7 SMMR and DMSP SSM/I-SSMIS Passive Microwave Data, Version 1. National Snow and Ice Data Center, accessed 12 September 2017, https://doi.org/10.5067/8GQ8LZQVL0VL.

Cole, S. T., and J. Stadler, 2019: Deepening of the winter mixed layer in the Canada Basin, Arctic Ocean over 2006–2017. *J. Geophys. Res. Oceans*, **124**, 4618–4630, https://doi.org/10.1029/2019JC014940.

Davis, P. E. D., C. Lique, H. L. Johnson, and J. D. Guthrie, 2016: Competing effects of elevated vertical mixing and increased freshwater input on the stratification and sea ice cover in a changing Arctic Ocean. *J. Phys. Oceanogr.*, **46**, 1531–1553, https://doi.org/10.1175/JPO-D-15-0174.1.

Gallaher, S. G., T. P. Stanton, W. J. Shaw, S. T. Cole, J. M. Toole, J. P. Wilkinson, T. Maksym, and B. Hwang, 2016: Evolution of a Canada Basin ice-ocean boundary layer and mixed layer across a developing thermodynamically forced marginal ice zone. *J. Geophys. Res. Oceans*, **121**, 6223–6250, https://doi.org/10.1002/2016JC011778.

——, T. Stanton, W. Shaw, S.-H. Kang, J.-H. Kim, and K.-H. Cho, 2017: Field observations and results of a 1-D boundary layer model for developing near-surface temperature maxima in the Western Arctic. *Elementa*, **5**, 11, https://doi.org/10.1525/elementa.195.

Galley, R. J., B. G. T. Else, S. J. Prinsberg, D. Babb, and D. G. Barber, 2013: Sea ice concentration, extent, age, motion and thickness in regions of proposed offshore oil and gas development near the Mackenzie Delta – Canadian Beaufort Sea. *Arctic*, **66**, 105–116.

Gudkovich, Z. M., 1961: Relation of the ice drift in the Arctic Basin to ice conditions in Soviet Arctic seas (in Russian). *Tr. Okeanogr. Kom. Akad.*, **11**, 14–21.

Hakkinen, S., A. Proshutinsky, and I. Ashok, 2008: Sea ice drift in the Arctic since the 1950s. *Geophys. Res. Lett.*, **35**, L19704, https://doi.org/10.1029/2008GL034791.

Holloway, G., and Coauthors, 2007: Water properties and circulation in Arctic Ocean models. *J. Geophys. Res.*, **112**, C04S03, https://doi.org/10.1029/2006JC003642.

Hunkins, K., and J. A. Whitehead, 1992: Laboratory simulation of exchange through Fram Strait. *J. Geophys. Res.*, **97**, 11 299–11 322, https://doi.org/10.1029/92JC00735.

Hutchings, J. K., and M. K. Faber, 2018: Sea-ice morphology change in the Canada Basin summer: 2006–2015 ship observations compared to observations from the 1960s to the early 1990s. *Front. Earth Sci.*, **6**, 123, https://doi.org/10.3389/feart.2018.00123.

Ilıcak, M., and Coauthors, 2016: An assessment of the Arctic Ocean in a suite of interannual CORE-II simulations. Part III: Hydrography and fluxes. *Ocean Modell.*, **100**, 141–161, https://doi.org/10.1016/j.ocemod.2016.02.004.

Jackson, J. M., E. C. Carmack, F. A. McLaughlin, S. E. Allen, and R. G. Ingram, 2010: Identification, characterization, and change of the near-surface temperature maximum in the Canada Basin, 1993–2008. *J. Geophys. Res.*, **115**, C05021, https://doi.org/10.1029/2009JC005265.

Jin, M., J. Hutchings, Y. Kawaguchi, and T. Kikuchi, 2012: Ocean mixing with lead-dependent subgrid scale brine rejection parameterization in a climate model. *J. Ocean Univ. China*, **11**, 473–480, https://doi.org/10.1007/s11802-012-2094-4.

Kern, S., A. Rösel, L. Toudal Pedersen, N. Ivanova, R. Saldo, and R. Tage Tonboe, 2016: The impact of melt ponds on summertime microwave brightness temperatures and sea-ice concentrations. *Cryosphere*, **10**, 2217–2239, https://doi.org/10.5194/tc-10-2217-2016.

Kraus, E. B., and J. S. Turner, 1967: A one-dimensional model of the seasonal thermocline II. The general theory and its consequences. *Tellus*, **19**, 98–106, https://doi.org/10.3402/tellusa.v19i1.9753.

Krishfield, R., J. Toole, A. Proshutinsky, and M. L. Timmermans, 2008: Automated ice-tethered profilers for seawater observations under pack ice in all seasons. *J. Atmos. Oceanic Technol.*, **25**, 2091–2105, https://doi.org/10.1175/2008JTECHO587.1.

Kwok, R., 2018: Arctic sea ice thickness, volume, and multiyear ice coverage: Losses and coupled variability (1958–2018). *Environ. Res. Lett.*, **13**, 105005, https://doi.org/10.1088/1748-9326/aae3ec.

——, and D. A. Rothrock, 2009: Decline in Arctic sea ice thickness from submarine and ICESat records: 1958–2008. *Geophys. Res. Lett.*, **36**, L15501, https://doi.org/10.1029/2009GL039035.

——, G. Spreen, and S. Pang, 2013: Arctic sea ice circulation and drift speed: Decadal trends and ocean currents. *J. Geophys. Res. Oceans*, **118**, 2408–2425, https://doi.org/10.1002/jgrc.20191.

Lemke, P., 1987: A coupled one-dimensional sea ice-ocean model. *J. Geophys. Res.*, **92**, 13 164–13 172, https://doi.org/10.1029/JC092iC12p13164.

——, and T. O. Manley, 1984: The seasonal variation of the mixed layer and the pycnocline under polar sea ice. *J. Geophys. Res.*, **89**, 6494–6504, https://doi.org/10.1029/JC089iC04p06494.

Lique, C., 2015: Ocean science: Arctic sea ice heated from below. *Nat. Geosci.*, **8**, 172–173, https://doi.org/10.1038/ngeo2357.

Macdonald, R. W., E. C. Carmack, F. A. McLaughlin, K. K. Falkner, and J. H. Swift, 1999: Connections among ice, runoff and atmospheric forcing in the Beaufort Gyre. *Geophys. Res. Lett.*, **26**, 2223–2226, https://doi.org/10.1029/1999GL900508.

Martin, T., M. Steele, and J. Zhang, 2014: Seasonality and long-term trend of Arctic Ocean surface stress in a model. *J. Geophys. Res. Oceans*, **119**, 1723–1738, https://doi.org/10.1002/2013JC009425.

——, M. Tsamados, D. Schroeder, and D. L. Feltham, 2016: The impact of variable sea ice roughness on changes in Arctic Ocean surface stress: A model study. *J. Geophys. Res. Oceans*, **121**, 1931–1952, https://doi.org/10.1002/2015JC011186.

Martinson, D. G., 1990: Evolution of the Southern Ocean winter mixed layer and sea ice: Open ocean deepwater formation and ventilation. *J. Geophys. Res.*, **95**, 11 641–11 654, https://doi.org/10.1029/JC095iC07p11641.

——, and R. Iannuzzi, 1998: Antarctic ocean-ice interactions: Implications from ocean bulk property distributions in the Weddell Gyre. *Antarctic Sea Ice: Physical Processes, Interactions and Variability*, Antarctic Research Series, Vol. 74, Amer. Geophys. Union, 243–271, https://doi.org/10.1029/AR074p0243.

Maykut, G. A., and M. G. McPhee, 1995: Solar heating of the Arctic mixed layer. *J. Geophys. Res.*, **100**, 24 691–24 703, https://doi.org/10.1029/95JC02554.

McLaughlin, F. A., and E. C. Carmack, 2010: Deepening of the nutricline and chlorophyll maximum in the Canada Basin interior, 2003–2009. *Geophys. Res. Lett.*, **37**, L24602, https://doi.org/10.1029/2010GL045459.

——, E. Carmack, A. Proshutinsky, R. Krishfield, C. Guay, M. Yamamoto-Kawai, J. Jackson, and B. Williams, 2011: The rapid response of the Canada Basin to climate forcing. *Oceanography*, **24**, 146–159, https://doi.org/10.5670/oceanog.2011.66.

McPhee, M. G., 2012: Advances in understanding ice – Ocean stress during and since AIDJEX. *Cold Reg. Sci. Technol.*, **76–77**, 24–36, https://doi.org/10.1016/j.coldregions.2011.05.001.

——, and J. D. Smith, 1976: Measurements of the turbulent boundary layer under pack ice. *J. Phys. Oceanogr.*, **6**, 696–711, https://doi.org/10.1175/1520-0485(1976)006<0696:MOTTBL>2.0.CO;2.

——, T. P. Stanton, J. H. Morison, and D. G. Martinson, 1998: Freshening of the upper ocean in the Arctic: Is perennial sea ice disappearing? *Geophys. Res. Lett.*, **25**, 1729–1732, https://doi.org/10.1029/98GL00933.

Meneghello, G., J. Marshall, M. L. Timmermans, and J. Scott, 2018: Observations of seasonal up welling and downwelling in the Beaufort Sea mediated by sea ice. *J. Phys. Oceanogr.*, **48**, 795–805, https://doi.org/10.1175/JPO-D-17-0188.1.

——, ——, C. Lique, P. E. Isachsen, E. Doddridge, J. M. Campin, H. Regan, and C. Talandier, 2021: Genesis and decay of mesoscale baroclinic eddies in the seasonally ice-covered interior Arctic Ocean. *J. Phys. Oceanogr.*, **51**, 115–129, https://doi.org/10.1175/JPO-D-20-0054.1.

Morison, J., and J. D. Smith, 1981: Seasonal variations in the upper Arctic Ocean as observed at T-3. *Geophys. Res. Lett.*, **8**, 753–756, https://doi.org/10.1029/GL008i007p00753.

Newton, B., L. B. Tremblay, M. A. Cane, and P. Schlosser, 2006: A simple model of the Arctic Ocean response to annular atmospheric modes. *J. Geophys. Res.*, **111**, C09019, https://doi.org/10.1029/2004JC002622.

Nguyen, A. T., D. Menemenlis, and R. Kwok, 2009: Improved modeling of the Arctic halocline with a subgrid-scale brine rejection parameterization. *J. Geophys. Res.*, **114**, C11014, https://doi.org/10.1029/2008JC005121.

Nummelin, A., C. Li, and L. H. Smedsrud, 2015: Response of Arctic Ocean stratification to changing river runoff in a column model. *J. Geophys. Res. Oceans*, **120**, 2655–2675, https://doi.org/10.1002/2014JC010571.

Parkinson, C. L., J. C. Comiso, H. J. Zwally, W. N. Meier, and J. Stroeve, 2004: Nimbus-5 ESMR polar gridded sea ice concentrations, version 1. National Snow and Ice Data Center, accessed 16 September 2019, https://doi.org/10.5067/W2PKTWMTY0TP.

Peralta-Ferriz, C., and R. A. Woodgate, 2015: Seasonal and interannual variability of pan-Arctic surface mixed layer properties from 1979 to 2012 from hydrographic data, and the dominance of stratification for multiyear mixed layer depth shoaling. *Prog. Oceanogr.*, **134**, 19–53, https://doi.org/10.1016/j.pocean.2014.12.005.

Perovich, D. K., 2011: The changing Arctic sea ice cover. *Oceanography*, **24**, 162–173, https://doi.org/10.5670/oceanog.2011.68.

——, and J. A. Richter-Menge, 2015: Regional variability in sea ice melt in a changing Arctic. *Philos. Trans. Roy. Soc.*, **A373**, 20140165, https://doi.org/10.1098/rsta.2014.0165.

Petty, A., D. L. Feltham, and P. R. Holland, 2013: Impact of atmospheric forcing on Antarctic continental shelf water masses. *J. Phys. Oceanogr.*, **43**, 920–940, https://doi.org/10.1175/JPO-D-12-0172.1.

Polyakov, I. V., and Coauthors, 2020: Borealization of the Arctic Ocean in response to anomalous advection from sub-Arctic seas. *Front. Mar. Sci.*, **7**, 491, https://doi.org/10.3389/fmars.2020.00491.

Proshutinsky, A., and Coauthors, 2009: Beaufort Gyre freshwater reservoir: State and variability from observations. *J. Geophys. Res.*, **114**, C00A10, https://doi.org/10.1029/2008JC005104.

——, and Coauthors, 2019: Analysis of the Beaufort Gyre freshwater content in 2003–2018. *J. Geophys. Res. Oceans*, **124**, 9658–9689, https://doi.org/10.1029/2019JC015281.

Rampal, P., J. Weiss, and D. Marsan, 2009: Positive trend in the mean speed and deformation rate of Arctic sea ice, 1979–2007. *J. Geophys. Res.*, **114**, C05013, https://doi.org/10.1029/2008JC005066.

Randelhoff, A., I. Fer, and A. Sundfjord, 2017: Turbulent upper-ocean mixing affected by melt water layers during Arctic summer. *J. Phys. Oceanogr.*, **47**, 835–853, https://doi.org/10.1175/JPO-D-16-0200.1.

Reed, R. J., and B. A. Kunkel, 1960: The Arctic circulation in summer. *J. Meteor.*, **17**, 489–506, https://doi.org/10.1175/1520-0469(1960)017<0489:TACIS>2.0.CO;2.

Rosenblum, E., R. Fajber, J. C. Stroeve, S. T. Gille, L. B. Tremblay, and E. C. Carmack, 2021: Surface salinity under transitioning ice cover in the Canada Basin: Climate model biases linked to vertical distribution of fresh water. *Geophys. Res. Lett.*, **48**, e2021GL094739, https://doi.org/10.1029/2021GL094739.

Schauer, U., and M. Losch, 2019: Freshwater in the ocean is not a useful parameter in climate research. *J. Phys. Oceanogr.*, **49**, 2309–2321, https://doi.org/10.1175/JPO-D-19-0102.1.

Schweiger, A., R. Lindsay, J. Zhang, M. Steele, and H. Stern, 2011: Uncertainty in modeled Arctic sea ice volume. *J. Geophys. Res.*, **116**, C00D06, https://doi.org/10.1029/2011JC007084.

Sidorenko, D., and Coauthors, 2018: Influence of a salt plume parameterization in a coupled climate model. *J. Adv. Model. Earth Syst.*, **10**, 2357–2373, https://doi.org/10.1029/2018MS001291.

Spreen, G., R. Kwok, and D. Menemenlis, 2011: Trends in Arctic sea ice drift and role of wind forcing: 1992–2009. *Geophys. Res. Lett.*, **38**, L19501, https://doi.org/10.1029/2011GL048970.

Steele, M., W. Ermold, and J. Zhang, 2011: Modeling the formation and fate of the near-surface temperature maximum in the Canadian Basin of the Arctic Ocean. *J. Geophys. Res.*, **116**, C11015, https://doi.org/10.1029/2010JC006803.

Stroeve, J. C., and D. Notz, 2018: Changing state of Arctic sea ice across all seasons. *Environ. Res. Lett.*, **13**, 103001, https://doi.org/10.1088/1748-9326/aade56.

——, T. Markus, L. Boisvert, J. Miller, and A. Barret, 2014: Changes in Arctic melt season and implications for sea ice loss. *Geophys. Res. Lett.*, **41**, 1216–1225, https://doi.org/10.1002/2013GL058951.

Timmermans, M.-L., and P. Winsor, 2013: Scales of horizontal density structure in the Chukchi Sea surface layer. *Cont. Shelf Res.*, **52**, 39–45, https://doi.org/10.1016/j.csr.2012.10.015.

——, and J. Marshall, 2020: Understanding Arctic Ocean circulation: A review of ocean dynamics in a changing climate. *J. Geophys. Res. Oceans*, **125**, e2018JC014378, https://doi.org/10.1029/2018JC014378.

——, J. Toole, R. Krishfield, and P. Winsor, 2008: Ice-tethered profiler observations of the double-diffusive staircase in the Canada Basin thermocline. *J. Geophys. Res.*, **113**, C00A02, https://doi.org/10.1029/2008JC004829.

Tivy, A., S. E. Howell, B. Alt, S. McCourt, R. Chagnon, G. Crocker, T. Carrieres, and J. J. Yackel, 2011: Trends and variability in summer sea ice cover in the Canadian Arctic based on the Canadian Ice Service Digital Archive, 1960–2008 and 1968–2008. *J. Geophys. Res.*, **116**, C03007, https://doi.org/10.1029/2009JC005855.

Toole, J. M., M. L. Timmermans, D. K. Perovich, R. A. Krishfield, A. Proshutinsky, and J. A. Richter-Menge, 2010: Influences of the ocean surface mixed layer and thermohaline stratification on Arctic Sea ice in the central Canada Basin. *J. Geophys. Res.*, **115**, C10018, https://doi.org/10.1029/2009JC005660.

Tsamados, M., D. L. Feltham, D. Schroeder, D. Flocco, S. L. Farrell, N. Kurtz, S. W. Laxon, and S. Bacon, 2014: Impact of variable atmospheric and oceanic form drag on simulations of arctic sea ice. *J. Phys. Oceanogr.*, **44**, 1329–1353, https://doi.org/10.1175/JPO-D-13-0215.1.

——, ——, A. Petty, D. Schroder, and D. Flocco, 2015: Processes controlling surface, bottom and lateral melt of Arctic sea ice in a state of the art sea ice model. *Philos. Trans. Roy. Soc.*, **A373**, 20140167, https://doi.org/10.1098/rsta.2014.0167.

Turner, J., 1967: A one-dimensional model of the seasonal thermocline I. A laboratory experiment and its interpretation. *Tellus*, **19**, 88–97, https://doi.org/10.1111/j.2153-3490.1967.tb01461.x.

Untersteiner, N., A. S. Thorndike, D. A. Rothrock, and K. L. Hunkins, 2007: AIDJEX revisited: A look back at the U.S.-Canadian Arctic ice dynamics joint experiment 1970–78. *Arctic*, **60**, 327–336, https://doi.org/10.14430/arctic233.

Wadhams, P., 2012: New predictions of extreme keel depths and scour frequencies for the Beaufort Sea using ice thickness statistics. *Cold Reg. Sci. Technol.*, **76–77**, 77–82, https://doi.org/10.1016/j.coldregions.2011.12.002.

Yamamoto-Kawai, M., F. A. McLaughlin, E. C. Carmack, S. Nishino, K. Shimada, and N. Kurita, 2009: Surface freshening of the Canada Basin, 2003–2007: River runoff versus sea ice meltwater. *J. Geophys. Res.*, **114**, 2003–2007, https://doi.org/10.1029/2008JC005000.

Zhang, J., and M. Steele, 2007: Effect of vertical mixing on the Atlantic water layer circulation in the Arctic Ocean. *J. Geophys. Res.*, **112**, C04S04, https://doi.org/10.1029/2006JC003732.